

## Strain accumulation in the southern Alps (NE Italy) and deformation at the northeastern boundary of Adria observed by CGPS measurements

N. D'Agostino,<sup>1</sup> D. Cheloni,<sup>1</sup> S. Mantenuto,<sup>1</sup> G. Selvaggi,<sup>1</sup> A. Michelini,<sup>1</sup> and D. Zuliani<sup>2</sup>

Received 1 August 2005; accepted 31 August 2005; published 14 October 2005.

[1] We use continuous GPS observations to investigate the rate of strain accumulation in the area affected by the 1976 Friuli earthquakes. Comparison between the motion predicted by the rigid-rotation of Adria and the shortening observed across the study area suggests that the  $2.0 \pm 0.2$  mm/yr motion of Adria is entirely absorbed in the southern Alps through thrusting and crustal thickening with very little or no motion transferred to the north. We use elastic dislocation modelling to investigate the rate of interseismic loading and the geometry of the shear zone at depth. The best-fit solution indicates that a northward-dipping creeping dislocation, whose edge is located within a 50 km wide area beneath the southern Alps, accommodates  $2.1 \pm 0.5$  mm/yr of the Adria motion. Limited resolution on locking depth (acceptable values between 0 and 25 km) and trade-off between dip and slip do not allow a precise reconstruction of the dislocation geometry. The range of acceptable model parameters is consistent with a  $20^\circ$ -dipping dislocation, locked above 10 km depth and slipping at 2.4 mm/yr, whose geometry is suggested by seismological informations.

**Citation:** D'Agostino, N., D. Cheloni, S. Mantenuto, G. Selvaggi, A. Michelini, and D. Zuliani (2005), Strain accumulation in the southern Alps (NE Italy) and deformation at the northeastern boundary of Adria observed by CGPS measurements, *Geophys. Res. Lett.*, 32, L19306, doi:10.1029/2005GL024266.

### 1. Introduction

[2] Crustal thickening and mountain building in the eastern part of the southern Alps are determined by northward motion of the Adriatic block with respect to Eurasia [Calais *et al.*, 2002; Battaglia *et al.*, 2004; Serpelloni *et al.*, 2005]. Eulerian poles of rotation located in the western part of the Po Plain obtained using earthquake slip vectors and GPS velocities [Anderson and Jackson, 1987; Calais *et al.*, 2002], predict counter clockwise rotation of the Po Plain-Adriatic region and increasing convergence from the western to the eastern Alps (Figure 1). Historical seismicity and instrumentally recorded earthquakes, such as the 1976 Friuli earthquake sequence (main shocks,  $M_w = 6.4, 5.9, 6.0$  [Pondrelli and Ekström, 2001]), show thrust faulting on north-dipping low-angle faults in agreement with geological observations of active mountain building and active fold growing at the foothills of the southern Alps [Benedetti *et al.*, 2000; Galadini *et al.*, 2005]. In contrast, survey-style

GPS observations [Grenerczy, 2002; Grenerczy *et al.*, 2005] and seismotectonic studies [Hinsch and Decker, 2003], suggested that the Adria motion may be partly accommodated by lateral extrusion and strike-slip faulting in the Austrian Alps. Since these alternative seismotectonic scenarios have different implications for seismic hazard assessment, it is important to constrain the amount of Adria motion accommodated by lateral extrusion in the Austrian Alps and by thrusting in Friuli, respectively. In addition, the need for improved seismic hazard assessments in the highly populated and developed Po Plain region, requires the recognition of the active faults and the definition of their rates of interseismic loading. Here we report geodetic measurements, using continuous GPS (CGPS), of the rate of contraction across the eastern part of the southern Alps to define 1) the amount of Adria motion absorbed by thrusting and crustal thickening and 2) the rate of tectonic loading on the faults responsible for the 1976 Friuli earthquakes sequence.

### 2. CGPS Measurements

[3] Code and phase data for the time interval 1996.0–2005.5 have been reduced with the Gipsy-Oasis II software. Point positioning [Zumberge *et al.*, 1997] and precise orbits and clocks from JPL were used to analyse GPS data for sites in the deforming plate boundaries with ambiguity resolution for 4 sub-networks of 25–30 stations each. GPS sites on stable Eurasia are processed using precise point positioning and transformation parameters to ITRF2000 [Altamini *et al.*, 2002] from JPL (<ftp://sideshow.jpl.nasa.gov>). Daily solutions and associated covariance matrices for each subnetwork are then rotated and merged in a common reference frame defined by subtracting the rotation with respect to ITRF2000 of 24 stations on the non-deforming part of the Eurasia plate. We estimated the transformation for each day, on the basis of selected common stations that are present both in the Eurasia-fixed solution and in the daily ambiguity subnetworks solutions. On average seven common stations were present. Final time series in an Eurasian reference frame locally rotated to NEU components were simultaneously detrended and corrected for antenna jumps and annual and semi-annual sinusoidal signals. The velocity uncertainties account for both noncorrelated (white noise) and temporally correlated (flicker noise) site positions effects [Mao *et al.*, 1999; Dixon *et al.*, 2000].

### 3. Motion of the Adriatic Block

[4] To establish the motion of the Adriatic block with respect to Eurasia we estimate the rotation vectors which

<sup>1</sup>Istituto Nazionale Geofisica Vulcanologia, Roma, Italy.

<sup>2</sup>Centro Ricerche Sismologiche, Udine, Italy.

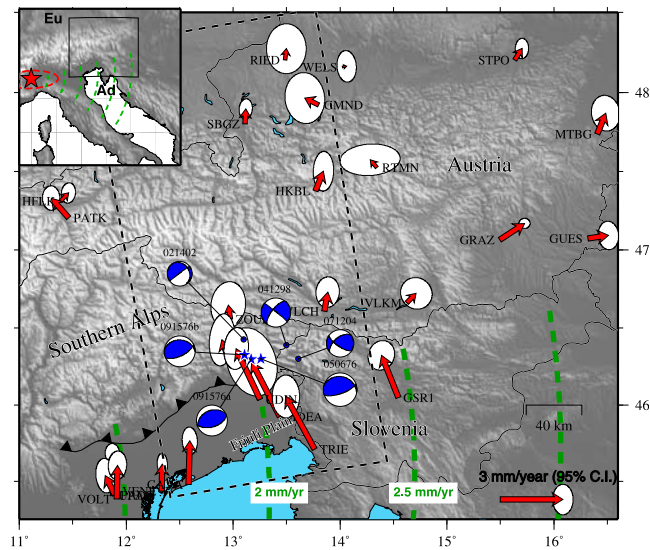


**Figure 1.** Seismotectonic map of the southern Alps with focal solutions from the RCMT database (<http://www.ingv.it/mednet>). Red arrows are Eurasia-fixed GPS velocities (ellipses 95% C.I.). The black line with triangles represents the southern Alps frontal thrust system. Locations of the 1976 seismic events are indicated by stars. Green dashed lines are small circles of constant velocity about the Adria-Eurasia pole of rotation. The black dashed line encloses the GPS sites whose velocities have been projected onto a N170 direction. The inset shows the pole of rotation (red star with 95% error ellipse) of Adria (Ad) with respect to Eurasia.

minimizes the residuals horizontal velocities. We first considered 12 sites located on the Po Plain and on the Adriatic side of the Apennines (P1 pole, Euler pole of rotations given in Table A2 and Table A3 of the auxiliary material<sup>1</sup>). We did not include those sites, located south of the Gargano promontory (MATE, CADM) which move independently from the northern part of the Adriatic region [Calais *et al.*, 2002; Battaglia *et al.*, 2004]. We also did not include MEDI which has a velocity significantly different with respect to nearby sites most likely related to local monument instability. The obtained pole of rotation is located in the western part of the Po plain near TORI site. If we exclude the GPS sites which provide more than 50% of the formal data importance [Minster *et al.*, 1974] and reinvert the remaining velocities, the modified Adria angular velocity vector (P2 pole) is not statistically different and predicts motion in the Friuli plain that differs by less than 0.25 mm/yr in velocity and 3° in azimuth from that predicted by the best fitting angular velocity vector. The prediction of the best fitting angular velocity vector are thus robust with respect to the information that is contributed by any single site velocity.

#### 4. Active Strain Accumulation in the Friuli Region

[5] The GPS velocities projected onto the N170 direction show a rate of contraction of  $\sim 2$  mm/yr between TRIE

<sup>1</sup>Auxiliary material is available at <ftp://ftp.agu.org/apend/g/L/2005GL024266>.

(Trieste), laying on the Adria block, and the sites on the northern side of the Alps which do not significantly move with respect to Eurasia (Figure 2). This shortening rate is statistically within the  $1\sigma$  uncertainty of the value predicted by the Adria-Eurasia rotation in the Friuli plain ( $2.0 \pm 0.2$  mm/yr), and suggests the complete accommodation of the Adria motion in the southern, most seismically active, part of the eastern Alps by thrusting and crustal thickening. The comparison between the GPS horizontal velocities and the topographic swath profile shows that the largest strain rate is localized along the front of the mountain belt as observed in other actively deforming regions. The observed shortening is also consistent with  $M \geq 6$  seismic activity located along the southern edge of the southern Alps [Galadini *et al.*, 2005]. Microseismic activity (Figure 3b) recorded by the Friuli local seismic network (<http://www.crs.ingv.it>), concentrates within a 20 km wide belt located beneath the mountain front and along an approximately 20°, northward-dipping crustal volume. The 1976 earthquake main shocks (Figure 3b) nucleated in the shallow part of the area affected by intense microseismicity at a centroid depth, constrained by body-wave modelling [Cipar, 1980], between 6 and 10 km, and ruptured on  $\sim 20^\circ$  north-dipping, fault planes [Pondrelli and Ekström, 2001]. Geological and seismological observations have been used by Aoudia *et al.* [2000] to infer shallow blind thrusting and anticlinal growth along the Susans-Tricesimo and Bernadia thrust faults, considered by the authors as responsible for the 1976 main shocks. The recent  $M_w$  4.9 Mount Sernio (14 February 2002) main shock and its sequence ruptured a fault segment at the northern boundary of the microseismicity belt at depth of about 13 km. These observations suggest that interseismic strain is loading the locked fault zone that ruptured during the 1976 earthquake sequence.

[6] East of the area struck by the 1976 earthquake, strike-slip faulting on NW-SE vertical planes [Bajc *et al.*, 2001], is

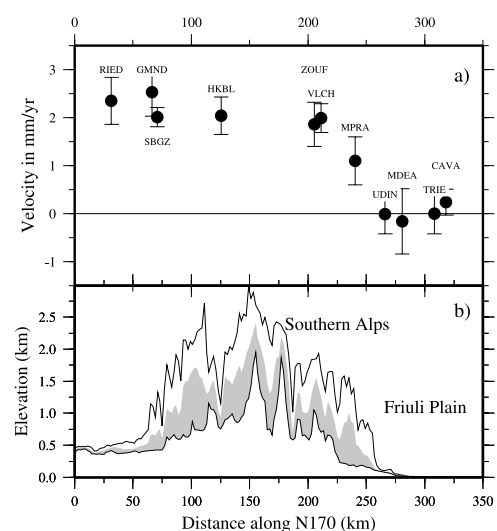


**Figure 2.** GPS and topographic data projected onto the N170 direction. (a) CGPS horizontal velocities (with  $1\sigma$  error bars) with respect to TRIE. (b) Maximum, minimum and average topographic data projected from a 20 km wide swath.

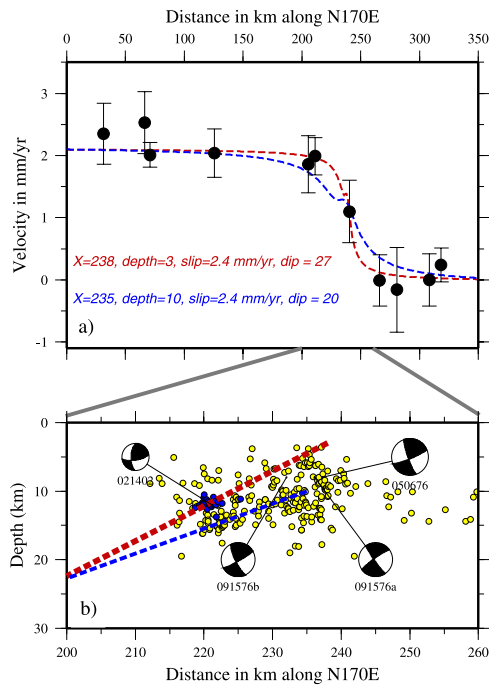


**Figure 3.** (a) Comparison of observations with predictions of dislocation models of reverse slip. The different models correspond to the best-fit solution (red,  $\phi^2 = 0$ ), and to an alternative solution (blue) consistent with model parameter uncertainties ( $\phi^2 = 0.17$ ), with distribution of microseismicity along a  $\sim N20^\circ$ -dipping zone, and with a fully-locked zone above 10 km. (b) Model geometry and seismicity. Yellow circles are seismic events recorded by the Friuli local seismic network. The 1994–2002 seismicity has been selected for vertical location errors  $<1$  km, horizontal location errors  $<0.5$  km and azimuthal gap  $<200^\circ$ . Also shown are focal mechanisms and location of the 1976 and 2002 events (associated minor events in blue).

consistent with the motion of the Adria block with respect to Eurasia. Whether the eastern boundary of the Adria block occurs on mapped active faults such as the Idrija fault [Bajc *et al.*, 2001] or it extends eastward is not clear. A significant northward motion of GSR1 in Slovenia with respect to Eurasia ( $2.2 \pm 0.3$  mm/yr to  $N22W$ ) suggests that most of the deformation is absorbed east of this site.

## 5. Dislocation Modelling

[7] We compared the observed horizontal velocities with the surface deformation accompanying slip on a two-dimensional planar north-dipping dislocation locked above a given depth (Figure 3a). The simplest model geometry includes four parameters: the fault slip rate, the dip angle and the horizontal and vertical positions of the fault tip. We sought the best-fitting values by systematically searching in the parameters space the values which minimize the  $\chi^2$  function ( $1/N \sum ((V_{calc} - V_{obs})/\sigma)^2$ ). To evaluate the range of model parameters that will satisfy the observations within their standard deviations we use the statistics defined by the  $\phi^2$  quantity ( $1/N \sum ((V_{calc} - V_{bf})/\sigma)^2$ ), where  $V_{bf}$  is the value predicted by the model parameters which minimize  $\chi^2$ . We estimate the uncertainty of model parameters from models

with  $\phi^2 \leq 1$ . Models for which  $\phi^2 \leq 1$  differ on average from the best-fitting model by an amount less than or equal to the observational accuracy of the data. The uncertainties of model parameters (Figure 4) show that (a) the tip of the creeping dislocation is located along the front of the southern Alps (distance along N170 =  $238 \pm 25$  km; (b) the locking depth is very poorly resolved and can be anywhere between 0 and 25 km (best fit solution at 3 km); (c) there is a complete trade-off between dip and slip on the creeping dislocation (best fit values  $27^\circ$  and 2.4 mm/yr respectively). The horizontal component of the slip on the fault (equal to  $slip \times \cos(dip)$ ) is however well resolved at  $2.1 \pm 0.5$  mm/yr. This value is very similar to the overall motion of the Adria block with respect to Eurasia. The geometry predicted by the best-fit solution is somehow contradictory with the distribution of background seismicity and with the depths of the 1976 events (Figure 3b) which would indicate complete locking above  $\sim 10$  km. Geodetic measurements and background seismicity can be potentially used jointly to delineate the creeping and locked portions of the fault, to provide important informations on the potential location and maximum size of future earthquakes. Figure 3 shows the best-fit together with an alternative solution that, while fitting the observations within the uncertainties ( $\phi^2 = 0.17$ ), is consistent with the background seismicity distribution and the hypocentral depths of the 1976 events.

## 6. Discussion and Conclusions

[8] The rate of shortening between the Friuli plain and the southern part of the eastern Alps shows that the motion of Adria is largely absorbed by thrusting and crustal thickening in Friuli and very little or no motion is rigidly transferred to the north in the Austrian Alps. This observation limits the amount of eastward rigid extrusion of the

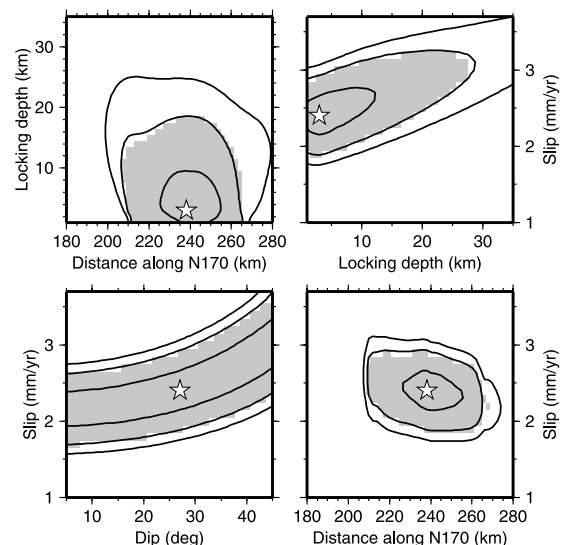


**Figure 4.** Each plot shows the variation of  $\chi^2$  as a function of two model parameters while the others are fixed at the values which minimize  $\chi^2$ . The white star indicates the best-fit solution. Contour lines delimit the 65%, 95% and 99% confidence interval respectively. The gray area corresponds to values with  $\phi^2 \leq 1$ , and indicates the range of acceptable values.

Austrian Alps along ENE left-lateral and ESE right-lateral faults [Grenerczy *et al.*, 2005] driven by the northward motion of Adria. Dislocation modelling constrains the tip of the creeping dislocation accommodating slip at depth, to be located in a 50 km-wide belt where active deformation and large  $M \geq 6$  earthquakes have been recognized. However, the sparse GPS observations in the actively shortening region do not allow us to resolve precisely the transition depth between the fully locked fault zone and the down-dip creeping section. A possible model, which uses the distribution of the background seismicity to map the geometry of the creeping dislocation and the depth of the 1976 events to constraint the locking depth, satisfies the observations within their uncertainties. In our interpretation, the current background seismicity maps the zone of brittle creep and interseismic straining in the velocity-strengthening portion of the fault zone between the fully ductile shear zone at depth (beneath the seismicity cut-off at  $\sim 18$  km) and the base of the locked fault zone where 1976-like seismic events nucleate [Perfettini and Avouac, 2004]. Slip on the creeping dislocation would cause strain to accumulate on the shallow locked section, a process expected to result in 1976-like earthquakes. At present we do not know what fraction of the deformation associated with loading on this structure is taken up seismically and which faults accommodate the observed shortening on the long-term. In particular, it is not clear whether the  $2.1 \pm 0.5$  mm/yr shortening is taken up only by the faults responsible for the 1976 sequence, or other unknown active faults are involved in the release of the elastic strain loaded by slip at depth. Future research will focus on the geometry of the creeping aseismic shear zone at depth, and on the role of the postseismic deformation following the 1976 Friuli sequence on the strain rate and background seismicity variations.

[9] **Acknowledgments.** We thank the Associate Editor Eric Calais and the reviewers, Christophe Vigny and Gyula Grenerczy, for constructive comments that helped to improve the manuscript.

## References

- Altamini, Z., P. Sillard, and C. Boucher (2002), ITRF2000: A new release of the International Terrestrial Reference Frame for Earth science applications, *J. Geophys. Res.*, *107*(B10), 2214, doi:10.1029/2001JB000561.
- Anderson, H., and J. Jackson (1987), Active tectonics of the Adriatic region, *Geophys. J. R. Astron. Soc.*, *91*, 937–983.
- Aoudia, A., A. Sarao', B. Bukchin, and P. Suhadolc (2000), The 1976 Friuli (NE Italy) thrust faulting earthquake: A reappraisal 23 years later, *Geophys. Res. Lett.*, *27*, 573–576.
- Bajc, J., A. Aoudia, A. Sara, and P. Suhadolc (2001), The 1998 Bovec-Krn mountain (Slovenia) earthquake sequence, *Geophys. Res. Lett.*, *28*, 1839–1842.
- Battaglia, M., M. H. Murray, E. Serpelloni, and R. Burgmann (2004), The Adriatic region: An independent microplate within the Africa-Eurasia collision zone, *Geophys. Res. Lett.*, *31*, L09605, doi:10.1029/2004GL019723.
- Benedetti, L., P. Tapponnier, G. C. P. King, B. Meyer, and I. Manighetti (2000), Growth folding and active thrusting in the Montello region, Veneto, northern Italy, *J. Geophys. Res.*, *105*, 739–766.
- Calais, E., J. M. Nocquet, F. Jouanne, and M. Tardy (2002), Current strain regime in the western Alps from continuous Global Positioning System measurements, 1996–2001, *Geology*, *7*, 651–654.
- Cipar, J. (1980), Teleseismic observations of the 1976 Friuli, Italy earthquake sequence, *Bull. Seismol. Soc. Am.*, *70*, 963–983.
- Dixon, T. H., M. Miller, F. Farina, H. Wang, and D. Johnson (2000), Present-day motion of the Sierra Nevada block and some tectonic implications for the Basin and Range province, North American Cordillera, *Tectonics*, *19*, 1–24.
- Galadini, F., M. E. Poli, and A. Zanferrari (2005), Seismogenic sources potentially responsible for earthquakes with  $M > 6$  in the eastern southern Alps (Thiene-Udine sector, NE Italy), *Geophys. J. Int.*, *160*, 1–24, doi:10.1111/j.1365-246X.2005.02571.x.
- Grenerczy, G. (2002), Tectonic processes in the Eurasian-African Plate Boundary Zone revealed by space geodesy, in *Plate Boundary Zones, Geodyn. Ser.*, vol. 30, edited by S. Stein and J. T. Freymuller, pp. 67–86, AGU, Washington, D. C.
- Grenerczy, G., G. Sella, S. Stein, and A. Kenyeres (2005), Tectonic implications of the GPS velocity field in the northern Adriatic region, *Geophys. Res. Lett.*, *32*, L16311, doi:10.1029/2005GL022947.
- Hirsch, R., and K. Decker (2003), Do seismic slip deficits indicate an underestimated earthquake potential along the Vienna Basin Transfer Fault System?, *Terra Nova*, *15*, 343–349.
- Mao, A., C. G. A. Harrison, and T. H. Dixon (1999), Noise in GPS coordinate time series, *J. Geophys. Res.*, *104*, 2797–2816.
- Minster, J. B., T. H. Jordan, P. Molnar, and E. Haines (1974), Numerical modeling of instantaneous plate tectonics, *Geophys. J. R. Astron. Soc.*, *36*, 541–576.
- Perfettini, H., and J. P. Avouac (2004), Stress transfer and strain rate variations during the seismic cycle, *J. Geophys. Res.*, *109*, B06402, doi:10.1029/2003JB002917.
- Pondrelli, S., and G. Ekström (2001), Seismotectonic re-evaluation of the 1976 Friuli, Italy, seismic sequence, *J. Seismol.*, *5*, 73–83.
- Serpelloni, E., M. Anzidei, P. Baldi, G. Casula, and A. Galvani (2005), Crustal velocity and strain-rate fields in Italy and surrounding regions: New results from the analysis of permanent and non-permanent GPS networks, *Geophys. J. Int.*, *161*, 861–880, doi:10.1111/j.1365-246X.2006.06218.x.
- Zumberge, J. F., M. B. Heflin, D. C. Jefferson, M. M. Watkins, and F. H. Webb (1997), Precise point positioning for the efficient and robust analysis of GPS data from large networks, *J. Geophys. Res.*, *102*, 5005–5018.
- N. D'Agostino, D. Cheloni, S. Mantenuto, A. Michelini, and G. Selvaggi, Istituto Nazionale Geofisica Vulcanologia, Via Vigna Murata 605, I-00143 Roma, Italy. (dagostin@ingv.it)
- D. Zuliani, Centro Ricerche Sismologiche, I-33100 Udine, Italy.